THE JOURNAL OF PHYSICAL CHEMISTRY B

ARTICLE

pubs.acs.org/JPCB

Orientational Dependence of the Affinity of Guanidinium Ions to the Water Surface

Erik Wernersson,*[,†] Jan Heyda,[†] Mario Vazdar,[†,‡] Mikael Lund,[§] Philip E. Mason,[∥] and Pavel Jungwirth[†]

[†]Institute of Organic Chemistry and Biochemistry, Academy of Sciences of the Czech Republic, and Center for Biomolecules and Complex Molecular Systems, Flemingovo nám. 2, 16610 Prague 6, Czech Republic

[‡]Division of Organic Chemistry and Biochemistry, Rudjer Bošković Institute, P.O. Box 180, HR-10002 Zagreb, Croatia

[§]Department of Theoretical Chemistry, Lund University, P.O. Box 124, SE-22100 Lund, Sweden

[∥]Department of Food Science, Stocking Hall, Cornell University, Ithaca, New York 14853, United States

Supporting Information

ABSTRACT: The behavior of guanidinium chloride at the surface of aqueous solutions is investigated using classical molecular dynamics (MD) simulations. It is found that the population of guanidinium ions oriented parallel to the interface is greater in the surface region than in bulk. The opposite is true for ions in other orientations. Overall, guanidinium chloride is depleted in the surface region, in agreement with the fact that the addition of guanidinium chloride increases the surface tension of water. The orientational dependence of the surface affinity of the guanidinium cation is related to its anisotropic hydration. To bring the ion to the surface in the parallel orientation does not require hydrogen bonds to be broken, in contrast to other orientations. The surface enrichment of parallel-oriented guanidinium indicates that its solvation is more favorable near the surface than in bulk solution for this orientation. The dependence of the bulk and surface properties of guanidinium on the force field parameters is also investigated. Despite significant quantitative differences between the force fields, the surface behavior is qualitatively robust. The implications for the orientations of the guanidinium groups of arginine side chains on protein surfaces are also outlined.

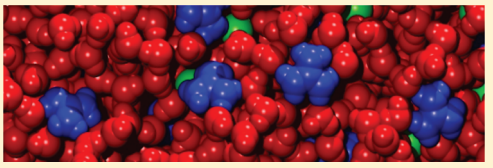

INTRODUCTION

The guanidinium cation ($C(NH_2)_3^+$) is composed of three amino groups bonded to a central carbon atom. Due to the conjugation of the nitrogen lone pairs with the empty p-orbital of the carbon atom, the ion is planar.[1] It can thus act as a hydrogen bond donor only along its edge. The faces of the guanidinium cation are poor hydrogen-bond acceptors due to the positive charge of the ion. Overall, the guanidinium−water interactions appear to be comparable to water−water interactions, with no signs of a strongly bound solvation shell detectable in either neutron scattering experiments or dielectric relaxation spectroscopy.[2,3] This does not, however, refute the observations from molecular dynamics (MD) simulations that there is significant ordering of water around the guanidinium hydrogens, as is visible in the spatial distribution function for free guanidinium ions as well as arginine guanidinium groups.[4,5] In contrast, the faces of the guanidinium ion do not order water to the same extent. The solvation shell of the guanidinium ion is thus heterogeneous, which makes the ion difficult to classify unambiguously in terms of its interaction with water.

Surface tension measurements indicate, via the Gibbs adsorption isotherm,[6] that the guanidinium cation is excluded from the air−water interface, but less so than small cations such as sodium.[7−10] Similar measurements for the water−mercury interface in the presence of guanidinium chloride indicate that guanidinium ions are adsorbed at that interface.[11] The situation at the metal−water interface, however, is different from that at the air−water interface in that attractive image and dispersion interactions act on the ions. Thermodynamic analysis of surface tension measurements can only give information about the total excess or deficiency of salt in the interfacial region.[6] Therefore, it cannot provide molecular insight without the introduction of model assumptions.

Guanidinium salts are widely used as protein denaturants and tend to solubilize both hydrophilic polyglycine, a model of the protein backbone, and hydrophobic, especially aromatic, amino acids.[12−14] It can be inferred from thermodynamic properties of protein solutions that guanidinium is enriched at the protein surface to an extent that is consistent with binding to both aromatic residues and backbone peptide groups.[15] There is, however, some ambiguity about the interpretation of the guanidinium interaction with the protein backbone in terms of direct hydrogen bonding to the amide carbonyl groups,[16] as previously proposed.[13]

Several computational studies on guanidinium salts, and the structurally related denaturant urea, have been carried out in recent years; see ref 17 for a recent review. The simulation of hydrophobic polymers, free from polar groups, shows that guanidinium chloride favors outstretched conformations.[18] This indicates that guanidinium weakens the net attraction between

Received: May 17, 2011
Revised: September 19, 2011
Published: October 10, 2011

monomers which is associated with the enrichment of guanidinium ions in the vicinity of the polymer.[18] The simulation of similar polymers in urea solution gives analogous results.[19] In that study, the strength of the dispersion forces between the polymer and urea was systematically varied. It was found that sufficiently strong dispersion interactions were necessary for urea to be preferentially enriched close to the polymer.[19] The simulation of capillary evaporation between two plates shows that the presence guanidinium chloride and, to a smaller extent, urea shifts the onset of capillary evaporation to smaller plate separation.[20] This is indicative of a stabilization of the liquid water between the plates by guanidinium ions, which were found to preferentially orient parallel to the plates.

The guanidinium motif is important in biochemistry also as part of the side chain of the amino acid arginine. Interestingly, oligomers of arginine have the ability to pass through the cell membranes of living cells, with a maximum in penetrating efficiency between the nona- and pentadecamer.[21] This property is shared both with some peptides rich in arginine and synthetic polymers containing the guanidinium moiety, but not with oligolysines of comparable size.[22,23] As the cell-penetrating ability of the peptide penetratin is enhanced when lysine residues are replaced with arginine,[24] it is clear that the guanidinium motif promotes penetration. Also, some transmembrane ion channel proteins have domains rich in arginine residues, which act as voltage sensors across the cell membrane.[25] MD simulations indicate that the guanidinium side-chain groups of the voltage sensor domain of the KvAP K^+ channel protein in a phospholipid bilayer form a hydrogen-bonded network with water molecules and lipid phosphate groups that significantly distort the bilayer.[26]

To understand the behavior of the guanidinium group near complex, biologically relevant surfaces, it is useful to first comprehend its interaction with the simplest aqueous interface conceivable—the water surface. To this end, we have performed MD simulations of atomistic models of the guanidinium chloride solution surface. These simulations indicate that guanidinium ions are attracted to the water surface if oriented parallel to it, but repelled for other orientations.

COMPUTATIONAL DETAILS

Some of the force fields for the guanidinium ion used in the literature give contradictory results for the bulk structure of guanidinium chloride solutions.[4,27] For this reason we critically re-evaluated these force fields on the basis of the experimental chemical potential of the salt in solution; see Supporting Information (SI). This quantity is exceptionally well-suited for force field validation because the deviation from ideality of the chemical potential depends sensitively on the balance between ion−solvent and ion−ion interactions. Neither force field was found to be entirely satisfactory. An acceptable force field could, however, be obtained by modifying the molecular geometry and charge distribution of the guanidinium force field from ref 27 on the basis of ab initio calculations; see Table 1. The geometry in the original force field was taken from guanidinium chloride crystals.[28] As a result of the considerable strain due to the electrostatic interactions in the crystal, the equilibrium H−N−H angle in this force field was chosen as too wide. This, in turn, resulted in excessive guanidinium−chloride ion pairing because the N−H bonds on adjacent nitrogens were tilted toward each other, creating a favorable "binding site" for chloride. In contrast to the other models considered, the modified version of the force field in ref 27 presented here was capable of reproducing the concentration dependence of the chemical potential without contradicting existing spectroscopic data. We emphasize that our modifications of this force field should be construed as criticism of ref 27 only with respect to the unrealistic choice of the H−N−H angle. The parametrization strategy employed in that work is methodologically sound and would likely have yielded a realistic model of the guanidinium cation if a molecular geometry pertinent to the solution and not to the crystal had been adopted. The modified force field is used in all calculations presented below.

Table 1. Force Field Parameters for Guanidinium Chloride

Distances[a]	r_0(Å)	k_B (kJ/mol/Å^2)	
C−N	1.340	1935	
N−H	1.012	constrained	
Angles[b]	θ_0	k_A (kJ/mol/rad^2)	
N−C−N	120.00°	670.0[c]	
C−N−H	121.25°	390.0[c]	
H−N−H	117.50°	445.0[c]	
Non-Bonded Parameters[d]	σ (Å)	ε (kJ/mol)	Charge (e_0)
C	3.77[c]	0.417[c]	0.9961
N	3.11[c]	0.500[c]	−0.9493
H	1.58[c]	0.088[c]	0.4753
Cl	4.40[c]	0.470[c]	−1.0000
Dihedrals[e]	k_D (kJ/mol)		
N−C−N-H	40.1		
Improper Dihedrals[f]	k_I (kJ/mol/rad^2)		
N−N−C-N	167.2		

[a] $U_B = k_B(r - r_0)^2$. [b] $U_A = k_A(\theta - \theta_0)^2$. [c] Same as in ref 27. [d] Lennard−Jones form; geometric combination rules. [e] $U_D = k_D(1 - \cos 2\phi)$. [f] $U_I = k_I\theta^2$.

Simulations of the surface of guanidinium chloride solutions were performed in the geometry of a liquid slab. The system contained either 38 or 190 guanidinium and chloride ions and 1977 water molecules per unit cell, corresponding to molal concentrations of 1.1 and 5.3 m, respectively. The slab thickness was approximately 5 nm for the lower concentration and 6.5 nm for the higher concentration. Each slab was enclosed in a box with approximate dimensions of 4 × 4 × 15 nm, held constant during the simulations. The system was constructed such that the slab surface was parallel to the $x-y$ plane. The initial configurations were generated from the final frame of a bulk simulation by elongating the box z-axis, essentially cutting a slice from the bulk solution. After a 0.5 ns equilibration, the MD trajectories were propagated for 100 ns for the lower concentration and 50 ns for the higher concentration. Such long simulation times were required to fully converge the orientationally resolved density profiles (see below). The temperature was kept constant at 300 K using a Berendsen thermostat.[29] The cutoff for short-range interactions was 10 Å. Long-range electrostatic interactions were accounted for using particle-mesh Ewald summation with a grid spacing of approximately 1 Å.[30] In all cases, a time step of 1 fs was employed. The simulations were carried out using the AMBER 11 program package.[31]

ANALYSIS DETAILS

Since the guanidinium cation is far from being spherically symmetric, the orientation of the ion is important for its

interaction with water and other species. The orientation of the guanidinium cation relative to the water surface is quantified here as the angle θ (from 0 to 90°), between the normal to the guanidinium cation face and the box z-axis, which is perpendicular to the slab surface. Since the guanidinium model considered here is flexible and, therefore, only approximately planar in any given frame of the simulation, the guanidinium normal is taken as the normalized vector product of two of the three carbon−nitrogen vectors. All other orientational degrees of freedom are thus averaged out. We define the orientationally resolved density profile $g(z,\theta)$ as the local concentration of ions with orientation θ with the carbon atom at position z, normalized by the area element associated with θ and the bulk concentration to approach unity in bulk solution for all θ. The potential of mean force for a (hypothetically) constrained ion with a given, fixed orientation is given by

$$\omega(z,\theta) = -k_B T \ln g(z,\theta) \quad (1)$$

This quantity is analogous to the orientationally averaged potential of mean force and can be related to the difference in excess chemical potential between different z-positions for a given orientation θ. The relation between the concentration profile and the excess chemical potential underlines the importance of using a force field that reproduces this quantity in bulk solutions with reasonable accuracy.

Also the conditional concentration profile of water given the presence of a guanidinium ion at a fixed position with a fixed orientation is considered. If all orientational degrees of freedom except the θ-angle for the central guanidinium ion, taken to be located at z', are averaged out, this function can be written in terms of four coordinates as $g_w(\rho,z|z',\theta)$ where $\rho = (x^2 + y^2)^{1/2}$ is the radial distance from the central ion in the plane of the surface. This function has a precise statistical-mechanical meaning and may be thought of as the product between the water concentration profile and a partial coarse graining of the guanidinium−water pair distribution function.[32] Again, this density profile is normalized to the bulk concentration. To quantify the solvation of optimally positioned and oriented guanidinium ion, as seen below, the density profile $g_w(\rho,z|z',\theta)$ of water around such ions was considered. To allow sufficient statistics to be extracted from the simulation, the (further) coarse grained quantity

$$g_w(\rho,z) = \frac{\int_{z'_a}^{z'_b} dz' \int_1^{0.95} d\cos\theta \; g_w(\rho,z|z',\theta)}{\int_{z'_a}^{z'_b} dz' \int_1^{0.95} d\cos\theta} \quad (2)$$

is calculated in practice.

To quantify the hydrogen bonding as a function of depth, we have calculated the number of hydrogen bonds with water and chloride per guanidinium ion as a function of the z-coordinate (here, the guanidinium orientation was not taken into account). A water oxygen atom was taken as participating in a hydrogen bond if it was within 3.5 Å of a guanidinium nitrogen and within 2.45 Å of the guanidinium hydrogen and the angle between the guanidinium nitrogen−hydrogen bond and the line connecting the guanidinium nitrogen with the water oxygen was smaller than 30°. The analogous criteria were used for water−water hydrogen bonds. For guanidinium−chloride hydrogen bonds the chloride−nitrogen and chloride−hydrogen distance criteria were 4 and 2.8 Å, respectively, taking the slightly larger size of chloride compared to water into account. The average number of hydrogen bonds per molecule is sensitive to small variations in the choice of these cut-offs, but the relative variation of this quantity with the z-position is not.

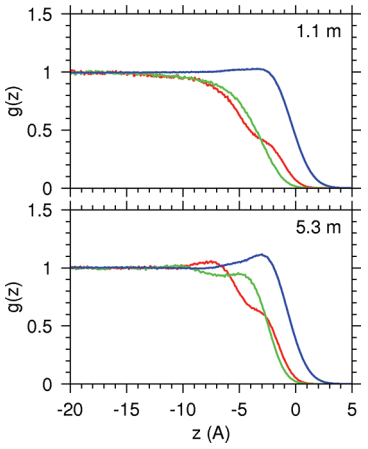

Figure 1. Density profiles of guanidinium carbon (red lines), chloride (green lines), and water oxygen (blue lines). In all cases, the Gibbs dividing surface for water is taken as the origin of the z-coordinate. The density profiles are normalized by the concentration in the middle of the slab. The statistical error of each point in the concentration profiles is about 2% for the lower concentration and about 1% as estimated by block averages.

RESULTS

The density profiles for guanidinium, chloride, and water are shown in Figure 1. The profiles are averages over the two equivalent halves of the slab. Both guanidinium and chloride are depleted from the interfacial region. There is, however, a shoulder at $z \approx -3$ Å (with $z = 0$ corresponding to the Gibbs dividing surface) in the guanidinium profiles. This feature is more pronounced for the higher concentration. For this concentration there is also a region of guanidinium enrichment in the subsurface. The smaller relative depletion at higher concentration is qualitatively consistent with the experimental observation that the surface tension of guanidinium chloride solutions increases sublinearly with concentration.[7]

The orientationally resolved guanidinium density profiles corresponding to the guanidinium profiles in Figure 1 are shown in Figure 2. Guanidinium ions are depleted at the surface for most orientations. The exceptions are those orientations where the ions are aligned parallel or nearly parallel to the surface, for which guanidinium ions are enriched around $z \approx -3$ Å relative to the bulk. This enrichment is larger at higher concentration. The shoulder in the orientation-averaged density profiles, Figure 1, is due to this enrichment of parallel-aligned guanidinium. That the guanidinium ions are adsorbed at the water surface trivially implies that there is a thermodynamic driving force for them to adsorb. From eq 1 the depth of the free energy minimum corresponding to the peak in $g(z, \theta)$ can be estimated as $-k_B T \ln(\max(g(z, \theta))$, that is, $-0.67\ k_B T$ for the lower concentration and $-1.25\ k_B T$ for the higher concentration. Similar calculations have been carried out for the force fields from refs 4 and 27; see the SI. The results are qualitatively similar for all force fields, but the height of the peak in $g(z, \theta)$ differ. That guanidinium is depleted from the interface in overall reflects the fact that the range of orientations for which guanidinium cations are repelled

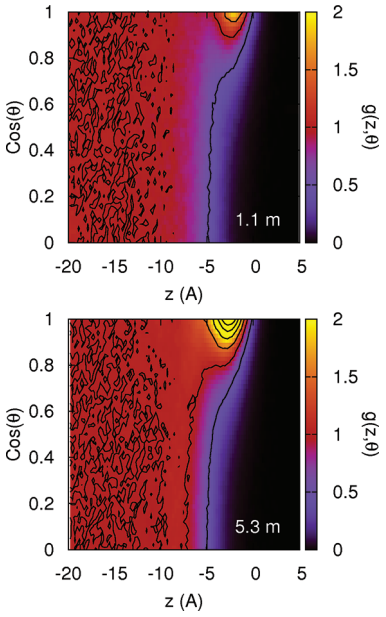

Figure 2. Color-enhanced contour plot of the angle resolved density profiles for guanidinium, $g(z,\theta)$. The contours are equidistant with a spacing of 0.5.

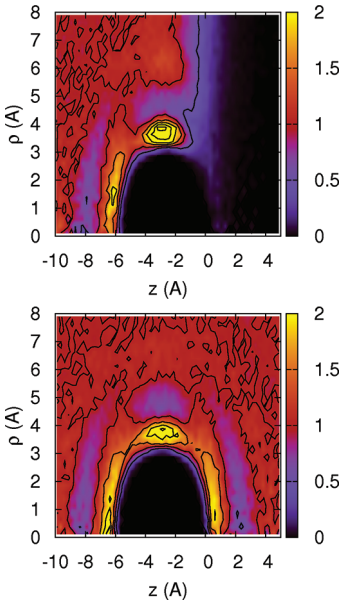

Figure 3. Color-enhanced contour plot of $g_w(\rho,z)$, essentially the concentration profile of water around an optimally positioned and oriented guanidinium cation. See the text for a precise definition. The corresponding quantity in bulk is also shown. Here, the z-origin is arbitrarily chosen to place the central guanidinium cation at the same z-coordinate as in the surface case for easy comparison. The contours are equidistant with a spacing of 0.5.

is overwhelmingly larger than than that for which they are attracted. This may be seen as reflecting the entropic cost of aligning guanidinium ions to the surface.

$g_w(\rho, z)$ is shown in Figure 3. z_a' and z_b' in eq 2 are chosen as −2.80 and −2.55 Å, respectively, bracketing the peak in $g(z, \theta)$. For reference, an analogous plot is constructed for the water distribution around guanidinium ions in bulk-like region in the middle of the slab. There, $g_w(\rho,z|z',\theta)$ is independent of z', and $g_w(\rho,z)$, therefore, only depends on $|z_b' - z_a'|$, which was chosen as 0.25 Å to enable comparison with the surface region. Two important differences between bulk and surface solvation are visible. First, the guanidinium face directed toward the vapor phase is almost completely desolvated at the surface. Second, there is an increase in the height of the peak corresponding water interacting with the edge of the interfacial guanidinium ion. The solvation structure is very similar to that in bulk solution in other respects.

The number of hydrogen bonds between guanidinium ions and water oxygen and chloride ions, respectively, per guanidinium ion are shown in Figure 4. The number of hydrogen bonds between guanidinium and water increases near the surface, as expected in light of Figure 3. The region in which this increase occurs roughly coincides with the location of the peak in the orientation resolved density profile, as in Figure 2. In the same region, there is a decrease in the number of hydrogen bonds between guanidinium and chloride and between water molecules. The number of water−guanidinium hydrogen bonds decreases with increasing concentration, while the difference in the number of such hydrogen bonds between the bulk and the surface regions increases with increasing concentration.

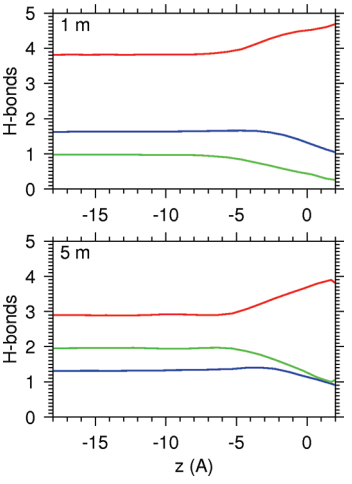

Figure 4. Number of hydrogen bonds between guanidinium ions and water molecules per guanidinium ions as a function of the z-coordinate (red curves) and the corresponding quantity for hydrogen bonds between guanidinium and chloride ions (green curves). The blue curves show the number of water−water acceptor hydrogen bonds per water molecule as a function of the z-coordinate.

DISCUSSION

It is remarkable that the partial desolvation of an ion can be associated with a free energy minimum, as is the case for the parallel-oriented guanidinium. The difference in surface affinity between guanidinium cations in the parallel and perpendicular orientations can be rationalized in terms of hydrogen bonding. For perpendicular-oriented guanidinium to be located at the depth corresponding to the peak in $g(z,\theta)$, in Figure 2, hydrogen bonds would have to be broken. In the parallel orientation, a guanidinium ion can be brought toward the surface while keeping a comparable number of hydrogen bonds in total as in bulk solution. For this orientation, only the face of the guanidinium

cation needs to be desolvated at the surface. Whether this desolvation of the face is actually favorable and drives the adsorption or merely is not disfavorable enough to prevent it cannot be discerned from the solvation structure alone. An alternative explanation, that is also compatible with the surface solvation structure, is that the hydrogen bonding environment near the surface is more favorable than in bulk.

A possible mechanism for the enrichment of parallel-oriented guanidinium is thus that the ion, thanks to its planar geometry, can take advantage of the hydrogen-bonding opportunities created by the deficit in hydrogen bonds between water molecules in the surface region. Since, on average, a smaller number of water−water hydrogen bonds has to be broken for each guanidinium−water hydrogen bond formed in the surface region than in the bulk solution, the net free energy gain from each guanidinium−water hydrogen bond should be larger near the surface. That the peak in $g_w(\rho,z)$ at $\rho \approx 4$ Å, $z \approx -3$ Å, shown in Figure 3, is slightly higher at the surface than in bulk is consistent with this proposed mechanism. It should be noted, however, that the loss of hydrogen bonding to chloride in the surface region should to some extent counteract this effect.

A connection can be made between the surface behavior of the guanidinium ions and their ability to form homo−ion pairs by stacking face to face, which is seen in simulations for several force fields.[4,33−36] There is also some recent experimental support for stacking interactions between guanidinium cations and arginine guanidinium groups.[37] Similar to the adsorption at the water surface in the parallel orientations, the stacked configuration requires desolvation of the faces. Apart from this desolvation, the balance of forces associated with stacking is different. The Coulomb repulsion between the ions is balanced by both dispersion interactions and the electrostatic interaction between higher multipoles, which can be attractive if the ions adopt a staggered configuration.[36] The observation of guanidinium−guanidinium stacking, however, is consistent with the notion that the magnitude of the free energy change associated with desolvation of the guanidinium faces is small in magnitude.

We are aware of no ion species that has a completely analogous structure to guanidinium. Urea can be regarded as a structural analogue, but this is a neutral compound. Nevertheless, there are some interesting analogies with other ions. One conspicuous example is the Eigen form of the hydronium cation.[38−40] This ion is weakly adsorbed at the water surface in an orientation with its hydrogens pointing toward the water bulk and the oxygen toward the vapor, though the strength of the adsorption is sensitive to the force field.[41] This orientational preference was rationalized by noting that the hydronium oxygen is a poor hydrogen-bond acceptor due to the positive charge of the ion.[38−40] Though the analogy with the guanidinium ion is not perfect, especially due to the fact that the hydronium ion is not planar, both ions may be regarded as "orientational amphiphiles" with respect to their hydrogen-bonding ability.

The flat, but negatively charged, nitrate ion shows an orientationally dependent depletion at the water surface but is not enriched for any orientation.[42] Note, however, that the latter conclusion is force-field dependent, and an earlier parametrization of this ion did show some surface enrichment.[43] In terms of its hydrogen-bonding ability, nitrate may be regarded as a "mirror image" of the guanidinium ion, with a similar geometry but the ability to accept, rather than donate, in-plane hydrogen bonds. It is unlikely that the same hydrogen-bonding structure would favor the solvation of both hydrogen bond donors and acceptors in the same region of the interface, since this situation would simply lead to favored water−water hydrogen bonding. The hydrogen bonds between water and the nitrate oxygens do not have the same orientational characteristics as the guanidinium−water hydrogen bonds. The conclusion about face desolvation at the surface is thus not directly generalizable from guanidinium to nitrate. The difference between the guanidinium and nitrate surface behavior is consistent with the notion that the water surface has a hydrogen-bonding structure that favors the solvation of planar hydrogen-bond donors.

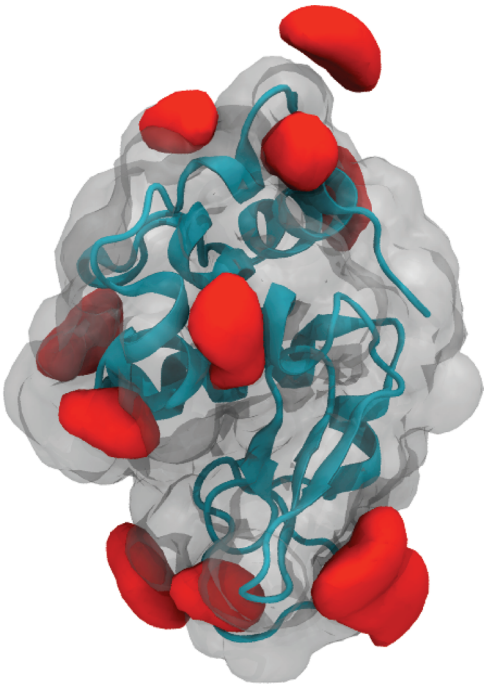

Figure 5. Spatial distribution of the guanidinium group on arginine side chains of hen-egg white lysozyme. The transparent gray iso-surface represents the average protein density (sans arginine side chains), while the red iso-surfaces represent the combined density of the three guanidinium nitrogens. The topmost density peak is for residue 128; see the text.

While no firm generalizations can be made to more complex systems at this stage, parallels between the guanidinium cation and the guanidinium motif of arginine can be drawn. A comprehensive database search of protein crystal structures has revealed that arginine side chains are frequently positioned and oriented in ways that are unexpected for a hydrophilic, cationic group.[44] This observation may be explained if the anisotropy in the solvation of the arginine guanidinium group is similar to that of the free guanidinium cation. The solvation of arginine may be favorable as long as the guanidinium moiety is exposed to water along its edge. Also the surface affinity of the arginine side chains may be similar to that of the guanidinium ion. As an example, we calculated the spatial distribution of the arginine side chains of lysozyme, as shown in Figure 5. The simulation details are given in the SI. Except for residue 128, located near the C-terminus in a region of high surface curvature, all arginine guanidinium groups tend to favor orientations parallel to the protein interface as seen by flat guanidinium iso-surfaces in close proximity to the protein surface. Further work toward quantifying the solvation of the guanidinium motif of arginine in the complex environment in the vicinity of a protein surface is under way and will be presented in a forthcoming publication.

CONCLUSIONS

The results presented above show that guanidinium ions tend to be enriched at the water surface if they are oriented parallel to it. The magnitude of this enrichment increases with increasing concentration. For the majority of orientations, the guanidinium ion is, however, predicted to be depleted in the surface region; therefore, the orientationally averaged density profile shows no net enrichment. The finding that parallel-oriented guanidinium ions are enriched at the surface, thus, does not contradict the experimental fact that guanidinium chloride shows a negative thermodynamic surface excess.[8−10] The orientational dependence of the surface propensity is explained in terms of the asymmetric solvation of the ion: In the parallel orientation, no hydrogen bonds have to be broken, and only the face of the ion has to be desolvated to bring the guanidinium cation to the interface. Furthermore, the structure of the water interface, in terms of hydrogen bonding and water orientation, may actually favor the solvation of parallel-oriented guanidinium compared to bulk. Work is underway to examine to what extent the conclusions about the surface solvation of the guanidinium ion are applicable also to more complex interfaces, such as the protein−water interface.

ASSOCIATED CONTENT

Supporting Information. Information about how the guanidinium chloride force field was constructed and validated, a comparison with two existing force fields, and a section describing how the lysozyme simulation was performed. This material is available free of charge via the Internet at http://pubs.acs.org.

AUTHOR INFORMATION

Corresponding Author
*E-mail: erik.wernersson@uochb.cas.cz.

ACKNOWLEDGMENT

P.J. thanks the Czech National Science Foundation (Grant 203/08/0114), the Ministry of Education (Grant LC512), and the Academy of Sciences (Praemium Academie) for support. For financial support, M.L. thanks the Swedish Research Council through the eSSENCE project and the Linneaus Center of Excellence "Organizing Molecular Matter".

REFERENCES

(1) Gund, P. *J. Chem. Educ.* **1972**, *49*, 100–103.
(2) Mason, P.; Nielson, G. W.; Dempsey, C. E.; Barnes, A. C.; Cruickshank, J. M. *Proc. Nat. Acad. Sci. U.S.A.* **2003**, *100*, 4557–4561.
(3) Hunger, J.; Niedermayer, S.; Buchner, R.; Hefter, G. *J. Phys. Chem. B* **2010**, *114*, 13617–13627.
(4) Mason, P. E.; Nielson, G. W.; Enderby, J. E.; Saboungi, M.-L.; Dempsey, C. E.; MacKerell, A. D., Jr.; Brady, J. W. *J. Am. Chem. Soc.* **2004**, *126*, 11462–11470.
(5) Hassan, S. A. *J. Phys. Chem. B* **2009**, *109*, 21989–21996.
(6) Lyklema, J. *Fundamentals of Interface and Colloid Science*, Vol. I: Fundamentals; Academic Press: New York, 1991.
(7) Breslow, R.; Guo, T. *Proc. Natl. Acad. Sci. U.S.A.* **1990**, *87*, 167–169.
(8) Kumar, A. *Fluid Phase Equilib.* **2001**, *180*, 195–204.
(9) Pegram, L. M.; Record, M. T., Jr. *J. Phys. Chem. B* **2007**, *111*, 5411–5417.
(10) Pegram, L. M.; Record, M. T., Jr. *J. Phys. Chem. B* **2008**, *112*, 9428–9436.
(11) Baugh, L. M.; Parsons, R. *Electroanal. Chem.* **1975**, *58*, 229–240.
(12) Greene, R. F., Jr.; Pace, C. N. *J. Biol. Chem.* **1974**, *249*, 5388–5393.
(13) Robinson, D. R.; Jencks, W. P. *J. Am. Chem. Soc.* **1965**, *87*, 2462–2470.
(14) Nozaki, Y.; Tanford, C. *J. Biol. Chem.* **1970**, *245*, 1648–1652.
(15) Lee, J. C.; Timasheff, S. N. *Biochemistry* **1974**, *13*, 257–265.
(16) Lim, W. K.; Rösgen, J.; Englander, W. *Proc. Natl. Acad. Sci. U.S. A.* **2009**, *106*, 2595–2600.
(17) England, J. L.; Haran, G. *Annu. Rev. Phys. Chem.* **2011**, *62*, 257–277.
(18) Godawat, R.; Jamadagni, S. N.; Garde, S. *J. Phys. Chem. B* **2010**, *114*, 2246–2254.
(19) Zangi, R.; Zhou, R.; Berne, B. J. *J. Am. Chem. Soc.* **2009**, *131*, 1535–1541.
(20) England, J. L.; Pande, V. S.; Haran, G. *J. Am. Chem. Soc.* **2008**, *130*, 11854–11855.
(21) Mitchell, J. D.; Kim, D. T.; Steinman, L.; Fathman, C. G.; Rothbard, J. B. *J. Peptide Res.* **2000**, *56*, 318–325.
(22) Derossi, D.; Chassaing, G.; Prochiantz, A. *Trends Cell Biol.* **1998**, *8*, 84–87.
(23) Pantos, A.; Tsogas, I.; Paleos, C. M. *Biochim. Biophys. Acta, Biomembr.* **2008**, *1778*, 811–823.
(24) Åmand, H.; Fant, K.; Nordén, B.; Esbjörner, E. K. *Biochem. Biophys. Res. Commun.* **2008**, *371*, 621–625.
(25) Bezanilla, F. *Physiol. Rev.* **2000**, *80*, 555–592.
(26) Freites, J. A.; Tobias, D. J.; von Heine, G.; White, S. H. *Proc. Natl. Acad. Sci. U.S.A.* **2005**, *102*, 15059–15064.
(27) Weerasinghe, S.; Smith, P. E. *J. Chem. Phys.* **2004**, *121*, 2180–2186.
(28) Haas, D. J.; Harris, D. R.; Mills, H. H. *Acta Crystallogr.* **1965**, *19*, 676–679.
(29) Berendsen, H. J. C.; Postma, J. P. M.; van Gunsteren, W. F.; DiNola, A.; Haak, J. R. *J. Chem. Phys.* **1984**, *81*, 3684–3690.
(30) Essmann, U.; Perera, L.; Berkowitz, M. L.; Darden, T.; Lee, H.; Pedersen, L. G. *J. Chem. Phys.* **1995**, *103*, 8577–8593.
(31) Case, D. A.; Darden, T. A.; Cheatham, T. E., III; Simmerling, C. L.; Wang, J.; Duke, R. E.; Luo, R.; Walker, R. C.; Zhang, W.; Merz, K. M.; Roberts, B.; Wang, B.; Hayik, S.; Roitberg, A.; Seabra, G.; Kolossváry, I.; Wong, K. F.; Paesani, F.; Vanicek, J.; Liu, J.; Wu, X.; Brozell, S. R.; Steinbrecher, T.; Gohlke, H.; Cai, Q.; Ye, X.; Wang, J.; Hsieh, M.-J.; Cui, G.; Roe, D. H.; Mathews, D. H.; Seetin, M. G.; Sagui, C.; Babin, V.; Luchko, T.; Gusarov, S.; Kovalenko, A.; Kollman, P. A. *AMBER 11*; University of California: San Francisco, CA, 2010.
(32) Hansen, J.-P.; McDonald, I. R. *Theory of Simple Liquids*; Academic Press: New York, 2006.
(33) Boudon, S.; Wipff, G.; Maigret, B. *J. Phys. Chem.* **1990**, *94*, 6056–6061.
(34) Soetens, J.-C.; Millot, C.; Chipot, C.; Jansen, G.; Ángyán, J. G.; Maigret, B. *J. Phys. Chem. B* **1997**, *101*, 10910–10917.
(35) No, K. T.; Nam, K.-Y.; Scheraga, H. A. *J. Am. Chem. Soc.* **1997**, *119*, 12917–12922.
(36) Vondrášek, J.; Mason, P. E.; Heyda, J.; Collins, K. D.; Jungwirth, P. *J. Phys. Chem. Lett.* **2009**, *113*, 9041–9045.
(37) Kubíčková, A.; Křížek, T.; Coufal, P.; Wernersson, E.; Heyda, J.; Jungwirth, P. *J. Phys. Chem. Lett.* **2011**, *2*, 1387–1389.
(38) Petersen, M. K.; Iyengar, S. S.; Day, T. J. F.; Voth, G. A. *J. Phys. Chem. B* **2004**, *108*, 14804–14806.
(39) Mucha, M.; Frigato, T.; Levering, L. M.; Allen, H. C.; Tobias, D. J.; Dang, L. X.; Jungwirth, P. *J. Phys. Chem. B* **2005**, *109*, 7617–7623.
(40) Petersen, P. B.; Saykally, R. J. *J. Phys. Chem. B* **2005**, *109*, 7976–7980.
(41) Jagoda-Cwiklik, B.; Cwiklik, L.; Jungwirth, P. *J. Phys. Chem. A* **2011**, *115*, 5881–5886.
(42) Thomas, J. L.; Roeselová, M.; Dang, L. X.; Tobias, D. J. *J. Phys. Chem. A* **2007**, *111*, 3091–3098.
(43) Salvador, P.; Curtis, J. E.; Tobias, D. J.; Jungwirth, P. *Phys. Chem. Chem. Phys.* **2003**, *5*, 3752–3757.
(44) Pednekar, D.; Tendulkar, A.; Durani, S. *Proteins* **2009**, *74*, 155–163.